

Supporting Information

© Copyright Wiley-VCH Verlag GmbH & Co. KGaA, 69451 Weinheim, 2018

Demonstration of Improved Effectiveness Factor of Catalysts Based on Hollow Single Crystal Zeolites

Céline Pagis, Frédéric Meunier, Yves Schuurman, Alain Tuel,* Mathias Dodin, Raquel Martinez-Franco, and David Farrusseng

Demonstration of improved effectiveness factor of catalysts based on hollow single crystal zeolites

Céline Pagis [a,b], Frederic Meunier [a], Yves Schuurman [a], Alain Tuel* [a], Mathias Dodin [b], Raquel Martinez-Franco [b] and David Farrusseng [a]

[a] Université de Lyon, Université Claude Bernard Lyon 1, CNRS, IRCELYON - UMR 5256, 2 Avenue Albert Einstein, 69626 Villeurbanne Cedex, France

[b] IFP Energies Nouvelles, Etablissement de Lyon, BP3, 69360 Solaize, France

Supporting Information

| | |
|---|----|
| 1. EXPERIMENTAL SECTION..... | 2 |
| 1.1. Samples synthesis and basic characterization | 2 |
| 1.2. Catalytic hydrogenation of cyclohexene | 7 |
| 2. INFLUENCE OF HEAT AND MASS TRANSFER | 9 |
| 3. KINETIC STUDIES | 10 |

1. EXPERIMENTAL SECTION

1.1. Samples synthesis and basic characterization

Table S1: *Chemical composition of Pt-containing bulk and hollow HY zeolites*

| Sample | Pt (wt. %) | Al (wt. %) | Si (wt. %) | Si/Al |
|---------------|-------------------|-------------------|-------------------|--------------|
| Hollow HY | 0.99 | 1.21 | 42.83 | 33.8 |
| Bulk HY | 0.99 | 0.90 | 43.91 | 47.1 |

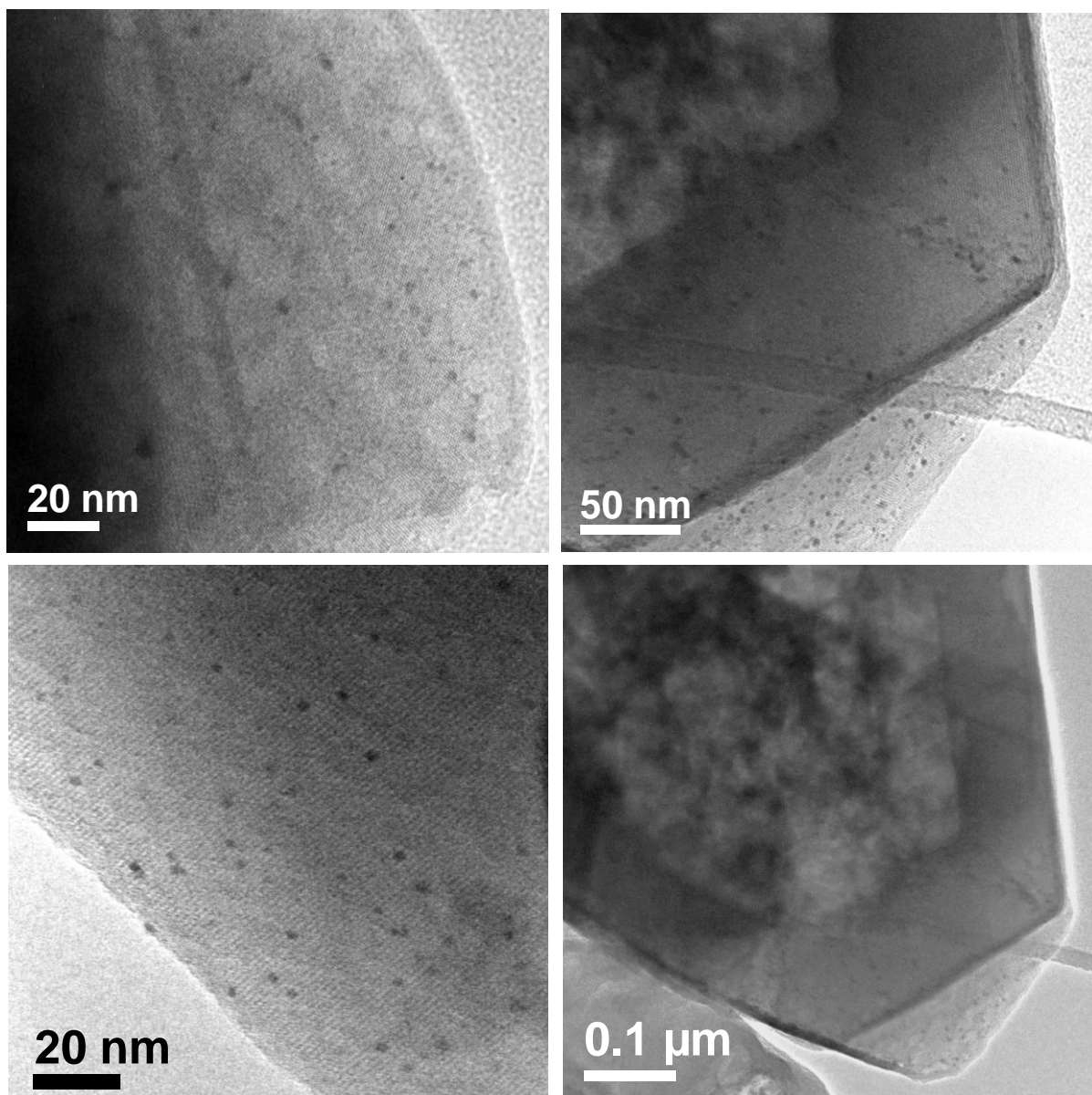


Figure S1. *Additional TEM images of hollow zeolite crystals and their embedded Pt nanoparticles.*

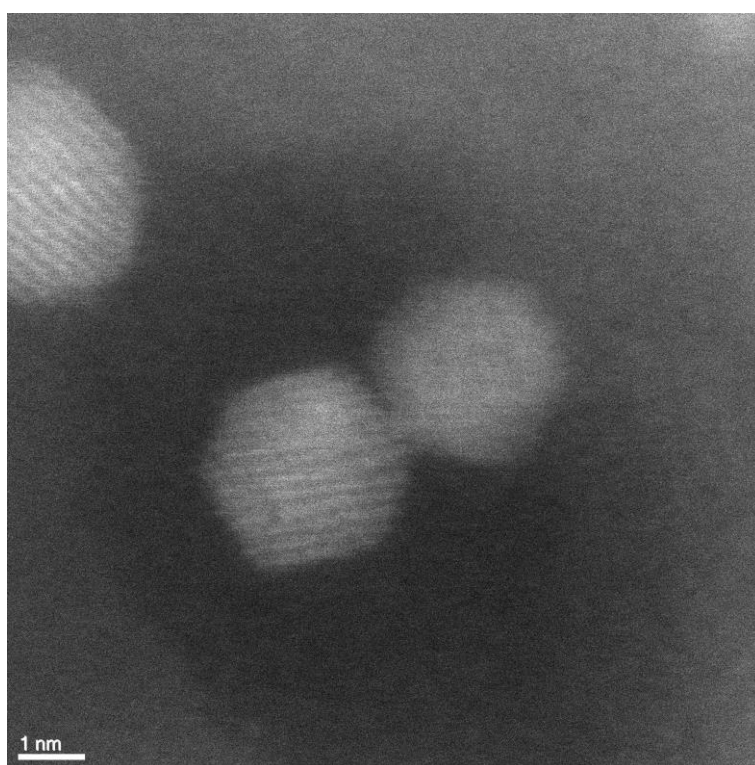
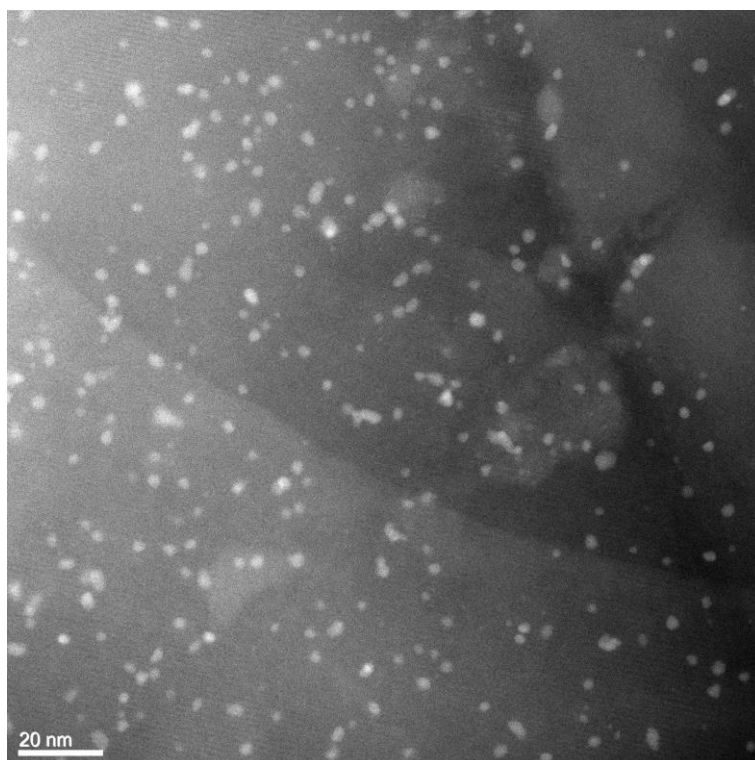


Figure S2. *STEM images of Pt nanoparticles in hollow NaY zeolite*

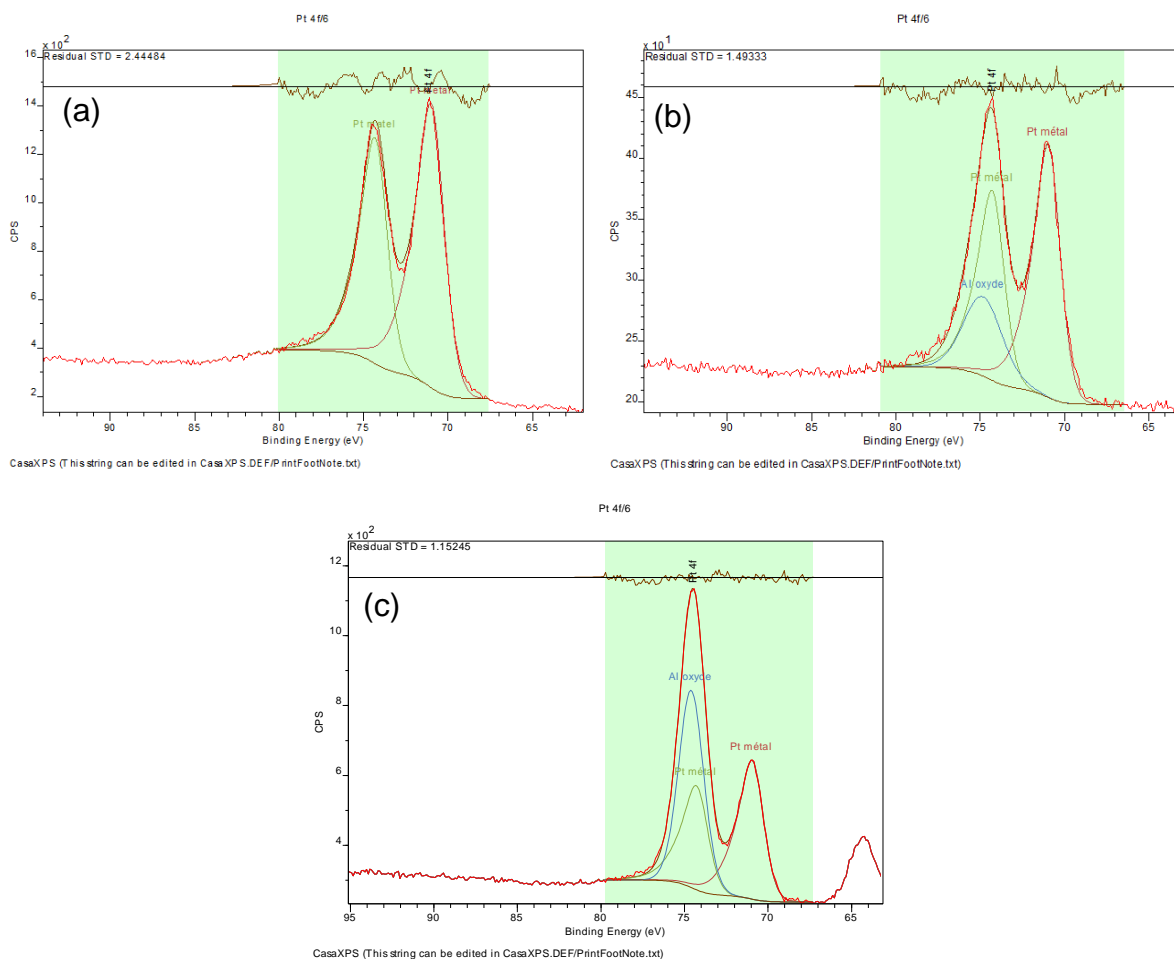


Figure S3. Pt 4f and Al 2p XPS spectra of Pt/SiO₂ (a), Pt@bulk HY (b) and Pt@hollow HY (c).

Table S2. Surface composition of Pt/SiO₂, Pt@bulk HY and Pt@hollow HY catalysts

| Samples | At. Concentration (%) | | | |
|--------------------------|-----------------------|------|-----|-------------------------|
| | O | Si | Pt | Other elements detected |
| 1.8 %Pt/SiO ₂ | 74.8 | 23.8 | 1.4 | - |
| 1% Pt@hollow HY | 76.8 | 23.1 | 0.1 | Al |
| 1% Pt@bulk HY | 75.2 | 24.7 | 0.1 | Al |

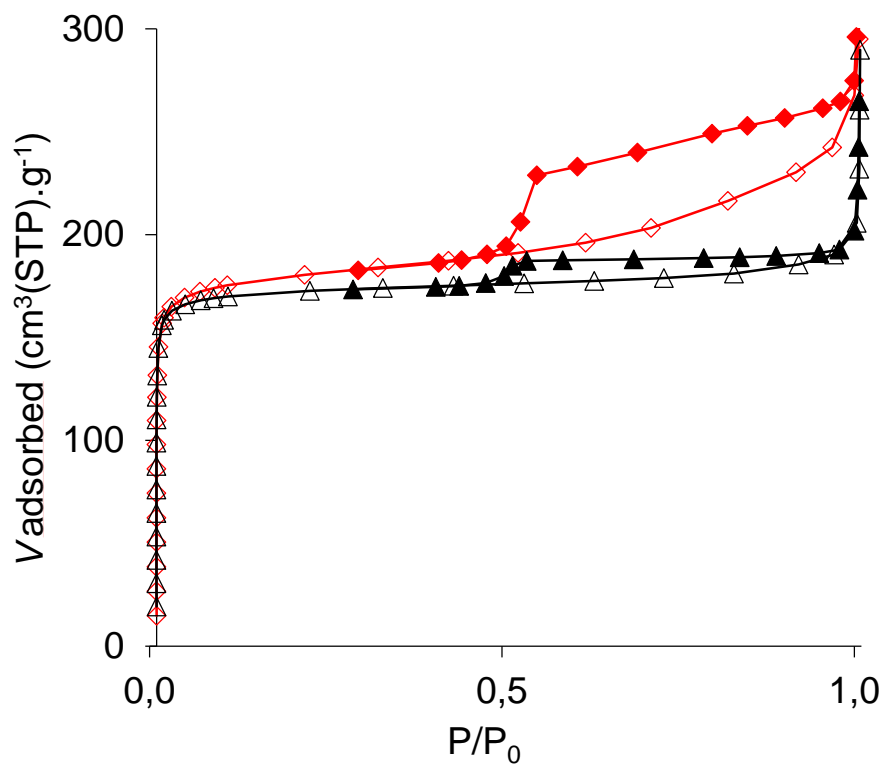


Figure S4. N_2 adsorption (open symbols) - desorption (filled symbols) isotherms on bulk (black) and hollow (red) zeolites before incorporation of platinum.

1.2. Catalytic Hydrogenation of Cyclohexene

Cyclohexene was received from Aldrich (purity > 99.0 %) and contained 100 ppm of BHT (2,6-Di-*tert*-butyl-4-methylphenol) as polymerization inhibitor. The hydrogenation tests were carried out using a tubular quartz plug flow reactor placed in a tubular furnace at atmospheric pressure. Precisely weighted masses of powder catalyst comprised between 9.5 and 10.5 mg were diluted in 100 mg of SiC. The catalyst and diluent were held between quartz wool plugs. Cyclohexene was fed using a saturator maintained at temperatures between 0.0°C and 18.0°C, leading to partial pressures of 3.3 kPa and 8.5 kPa, respectively. Due to the low concentration of BHT in the cyclohexene reagent and a high boiling point (i.e. 265 °C), it is assumed that the BHT concentration in gas-phase was negligible. Mixtures of high purity He and H₂ from Air Liquide (Alphagaz, 99.999% purity) further purified with using VICI® traps (models P-100-2 and P-200-2 for He and H₂, respectively) were flown through the cyclohexene saturator set at a suitable temperature to obtain the desired feed compositions. The proportion of reactant flow rates were varied to determine reaction orders, only using the data points obtained under differential conditions (less than 25% conversion). The total flow rate and temperature were possibly varied to ensure differential conditions. Cyclohexene conversion and cyclohexane production were determined through integration of the 3064-3000 cm⁻¹ and 1500-1400 cm⁻¹ spectral regions (Figure S5), calibration curves and a partial least square algorithm. Cyclohexane was the only product obtained with the experimental conditions used here. Traces of benzene could be observed only for temperatures above 200 °C.

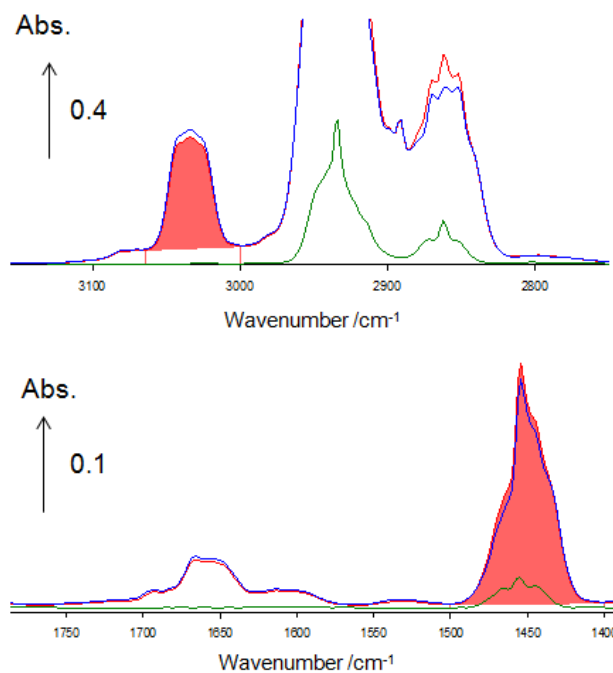


Figure S5. FT-IR transmission spectra recorded in the 10-cm path length gas cell during the hydrogenation of cyclohexene. The spectra in blue are that of the cyclohexene reagent. The red spectra were collected after the reactor at a conversion level of about 10%. The spectra in green were obtained by removing the contribution of the reactant (blue) from that of the reactor effluent (red) and corresponded exactly to that of cyclohexane. The areas of the bands highlighted in red between 3064-3000 cm^{-1} and 1500-1400 cm^{-1} were used to quantify cyclohexene and cyclohexane concentrations.

2. INFLUENCE OF MASS AND HEAT TRANSFER

In order to assess the influence of transport limitations on the intrinsic reaction rate, criteria have been derived that evaluate a $\pm 5\%$ deviation of the intrinsic rate with respect to the experimentally observed rate [1,2]. Kapteijn and Moulijn discuss extensively the different criteria and their usage [3]. Table S1 shows that all the criteria to assume ideal intrinsic kinetic conditions are fulfilled for all three samples, except the criteria for internal mass transfer for the zeolite based samples, **which are evaluated for each sample in detail in the main text and which was the objective of this study**. These criteria were evaluated at the highest reaction rate observed at 120°C.

Table S3. Evaluation of different criteria to assess the intrinsic kinetic conditions. For the calculations, the standard reaction conditions were used (see main text) and $r_{max} = 0.022 \text{ mol/kg}_{cat}/s$.

| Physical phenomenon | Criteria |
|--|-----------------------------------|
| plug flow (axial) | $h/d_p = 74 > 6$ |
| plug flow (radial) | $d_R/d_p = 27 > 10$ |
| degree of dilution (vol./vol.) | $0.91 < 0.97$ |
| external mass transfer (Carberry number) | $0.0005 < 0.05$ |
| internal mass transfer (Weisz-Prater) ^a | $1.4 \cdot 10^{-3} < 0.33$ |
| external heat transfer (film) | $0.03 \text{ K} < 1.1 \text{ K}$ |
| external heat transfer (radial) | $0.1 \text{ K} < 1.1 \text{ K}$ |
| internal heat transfer | $0.003 \text{ K} < 1.1 \text{ K}$ |

^a evaluated only for Pt/Al₂O₃. The zeolite based samples are treated in the main text.

3. KINETIC STUDIES

The absence of mass and heat transfer limitations in Pt/Al₂O₃ was evaluated through the appropriate criteria (Table S3). All catalysts exhibited similar apparent activation energies (Fig. S6, Table S4).

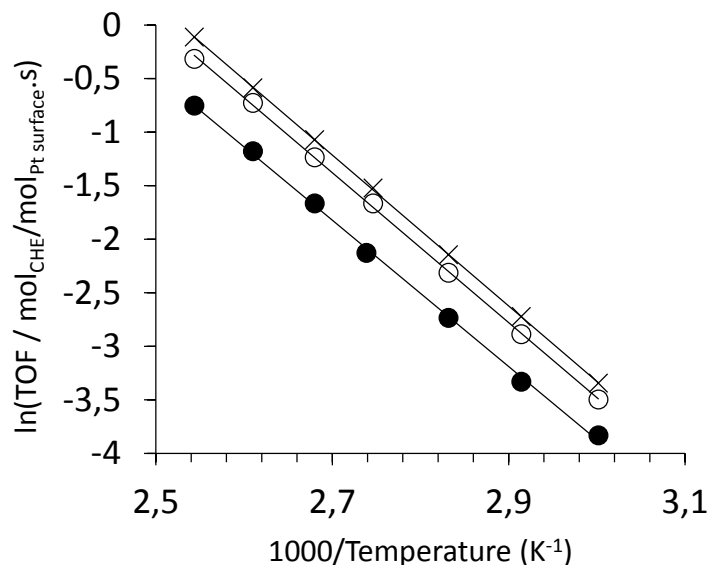


Figure S6. Arrhenius-type plot relating the natural logarithm of the apparent TOF versus the reciprocal temperature for (x) Pt/Al₂O₃, (●) Pt@bulk Y and (○) Pt@hollow Y. Feed = 3.3 % cyclohexene in H₂, total flow = 20 mL min⁻¹. The temperature was varied between 120 and 50°C.

Table S4. Kinetic Parameters.

| | E _{app} (kJ mol ⁻¹) | Partial order cyclohexene | Partial order H ₂ |
|-----------------------------------|---|------------------------------|------------------------------|
| Pt/Al ₂ O ₃ | 58.6 ± 0.2 | - 0.35 ± 0.02 | 0.98 ± 0.03 |
| Pt@bulk Y | 56.9 ± 0.8 | | 0.84 ± 0.05 |
| Pt@hollow Y | 58.0 ± 0.7 | | 0.94 ± 0.08 |

The negative hydrogenation reaction order with respect to cyclohexene determined in the case of Pt/Al₂O₃ is consistent with reaction self-poisoning by cyclohexene, which adsorbs strongly at the surface of Pt nanoparticles and hinders H₂ adsorption (Fig. S7, Table S4). The heat of adsorption of cyclohexene and H₂ on clean Pt(111) surfaces are actually 130 and 42 kJ mol⁻¹, respectively [4,5]. These data indicate that the platinum surface will be mostly covered with cyclohexene at reaction temperature.

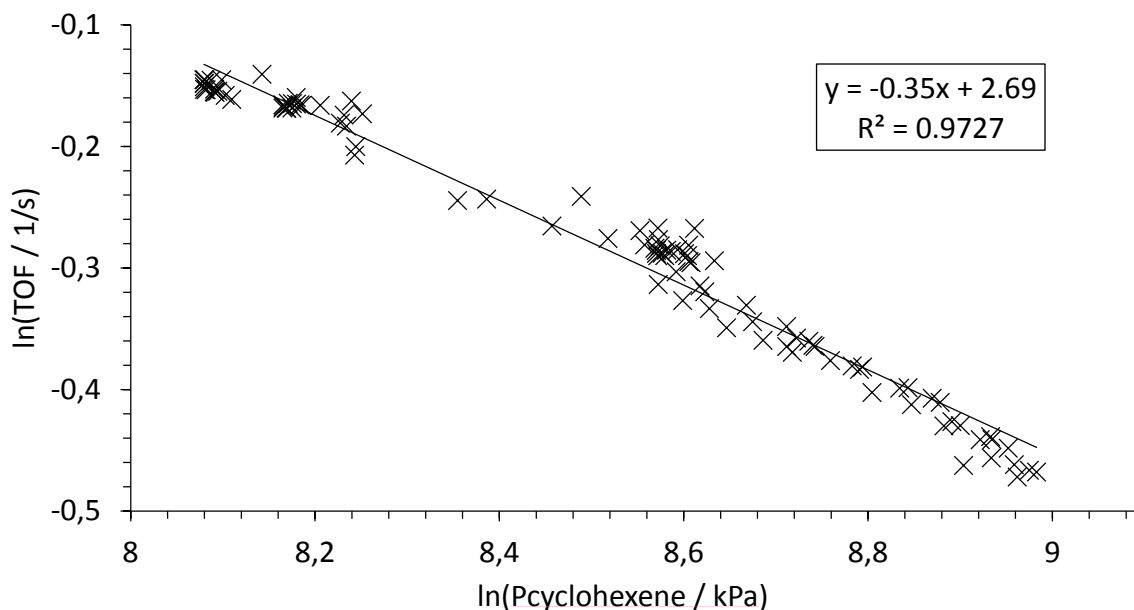


Figure S7. Plot relating the natural logarithm of the apparent TOF versus the natural logarithm the inlet cyclohexene partial pressure over Pt/Al₂O₃. Feed = 3.3 % < cyclohexene < 8.0 % in H₂, total flow = 20 mL min⁻¹. T = 120 °C.

In contrast, cyclohexane adsorption is weaker (ca. 36 kJ mol⁻¹) than that of H₂ and therefore the reaction product should only be present with a low coverage at reaction temperature and not limit adsorption of H₂ [6].

The H₂ reaction order is close to unity over Pt/Al₂O₃ and Pt@hollow Y, but slightly smaller on Pt@bulk Y, indicating that the reaction rate depends less on H₂ adsorption (Fig. S8, Table S2). This could be due to a lower apparent inhibition of H₂ adsorption due to a lower coverage of Pt by cyclohexene, resulting from a slower transport of cyclohexene to the Pt sites when encapsulated in bulk Y zeolite. It is thus expected that the bulk of the Pt@bulk Y catalyst will be richer than the reactor effluent in the reaction product cyclohexane, which adsorbs more weakly than H₂.

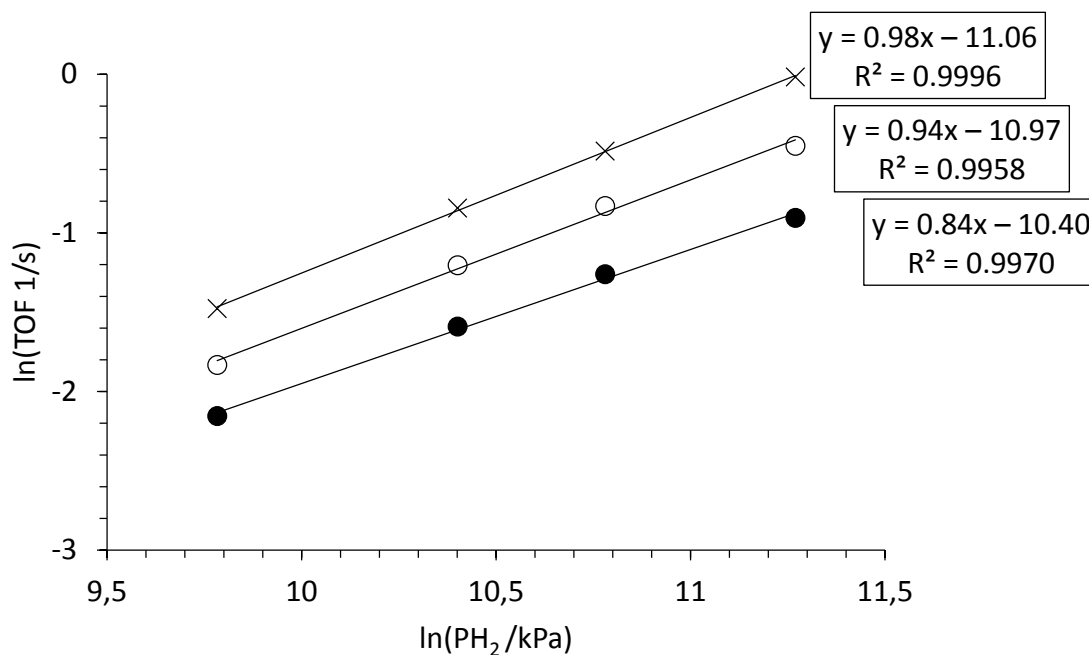


Figure S8. Plot relating the natural logarithm of the apparent TOF versus the natural logarithm of the inlet H₂ partial pressure over (x) Pt/Al₂O₃, (●) Pt@bulk Y and (○) Pt@hollow Y. The corresponding apparent reaction orders are noted near each curve.

- [1] D.E. Mears, Ind. Eng. Chem. Process Des. Dev., 1971, 10, 541.
- [2] C.N. Satterfield, Mass Transfer in Heterogeneous catalysis, MIT Press Cambridge, 1970.
- [3] F. Kapteijn, J.A. Moulijn, in: G.Ertl, H.Knözinger, J.Weitkamp (Eds.), Handbook of Heterogeneous Catalysis, Vol. 3, VCH, Weinheim, 1997, pp. 1359-1376.
- [4] O. Lytken, W. Lew, J. J. W. Harris, E. K. Vestergaard, J. M. Gottfried, C. T. Campbell, J. Am. Chem. Soc. 2008, 130, 10247–10257.
- [5] N. M. Marković, T. J. Schmidt, B. N. Grgur, H. A. Gasteiger, R. J. Behm, P. N. Ross, J. Phys. Chem. B 1999, 103, 8568–8577.
- [6] M. Saeys, M.-F. Reyniers, M. Neurock, G. B. Marin, Surf. Sci. 2006, 600, 3121–3134.